Supporting information 688

S1 File. GISAID acknowledgment table 689

S2 File GISAID accession IDs and metadata of the sequences used for 690
constructing genealogy 691

S3 File GISAID accession IDs and metadata of the sequences used in the 692
analysis of subclade frequency 693
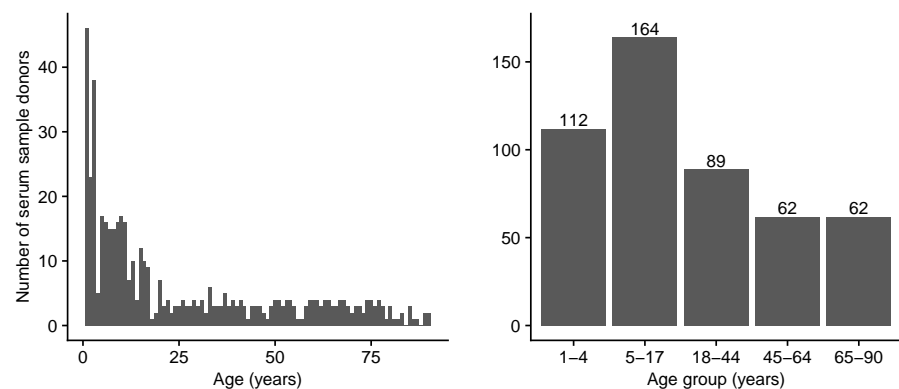
Supplementary Figures 694

Fig S1. Age distribution of serum sample donors. We collected serum samples
from May to August of 2017 from the University of Pennsylvania BioBank and
Children's Hospital of Philadelphia. The age distribution of donors at 1 year resolution
is shown on the left, and the sizes of different age groups are shown on the right.
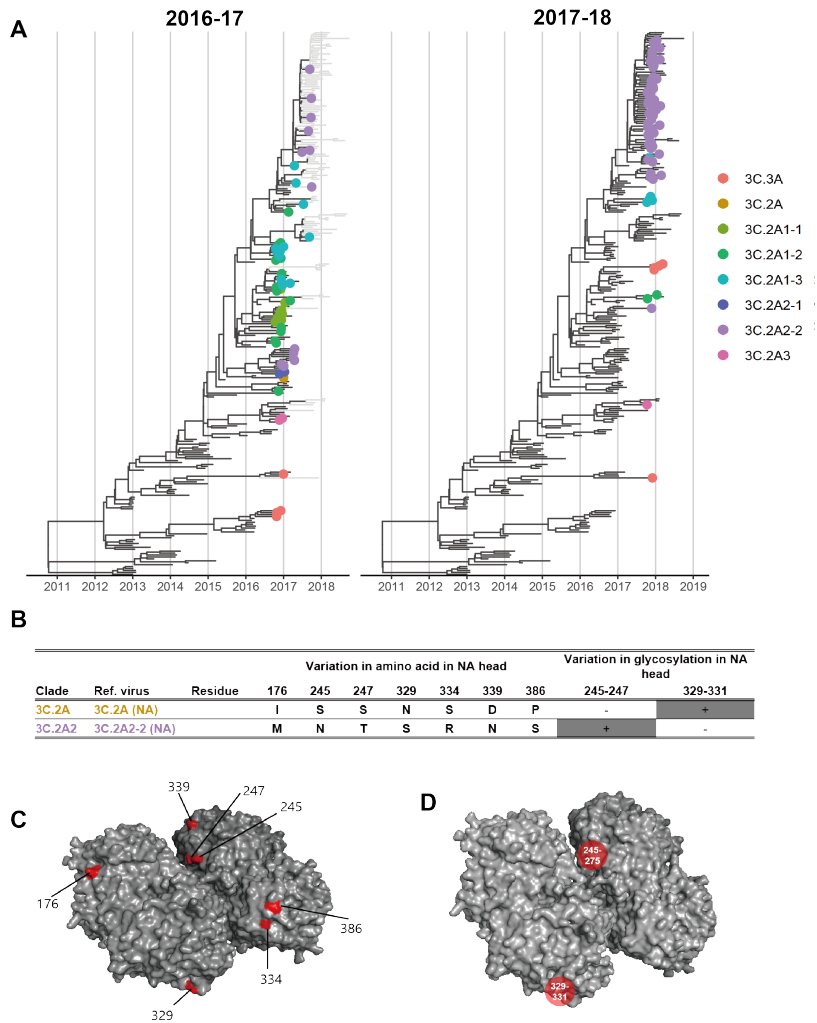
Fig S2. NA of co-circulating H3N2 clades during the 2016-17 and 2017-18 seasons. A. Genealogy of H3N2 showing NA sequence samples through the 2016-17 season (left) and through the 2017-18 season (right). Tips are filled circles if collected in North America during the 2016-17 season (left) and the 2017-18 season (right) and colored according to the associated test virus. B. Variable amino acids and PNGS between test viruses. Between clade 3C.2A (NA) and clade 3C.2A2 (NA), only substitutions at NA head are shown. C. The differences between clade 3C.2A (NA) and 3C.2A2-2 (NA) are shown on N2 head structure (Protein Data Bank: 6n4d). Amino acid differences between the two test viruses are colored in red. D. PNGS that vary between 3C.2A (NA) and 3C.2A2 (NA) are shown on the N2 structure.
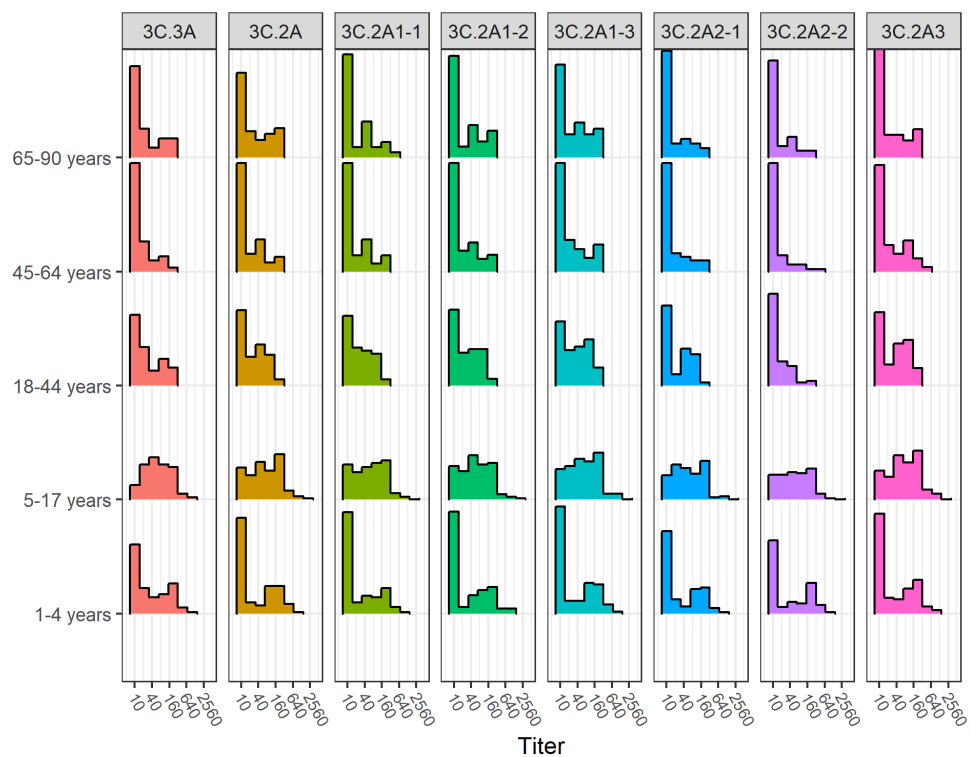
Fig S3. Distribution of HA titers for each strain by age group. A titer of 10 indicates the titer is below the limit of detection.
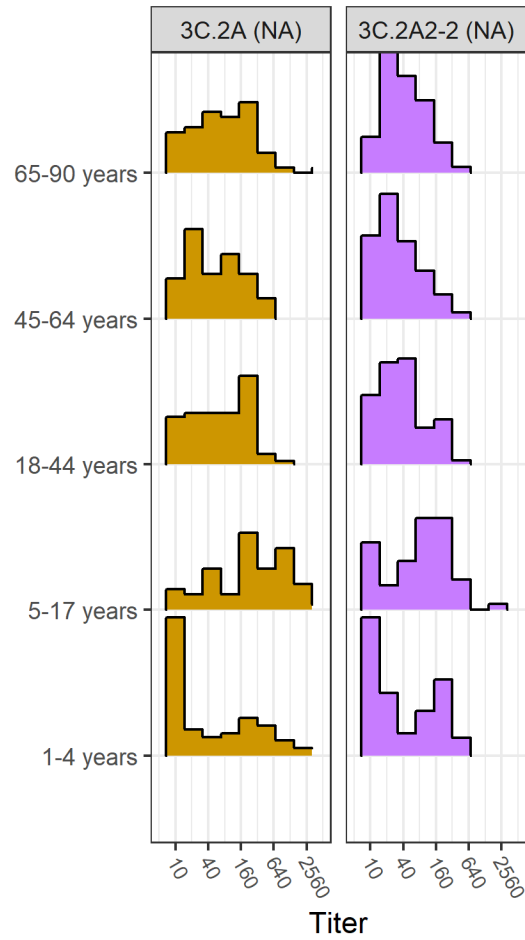
Fig S4. Distribution of NA titers for each strain by age group. A titer of 10 indicates the titer is below the limit of detection.
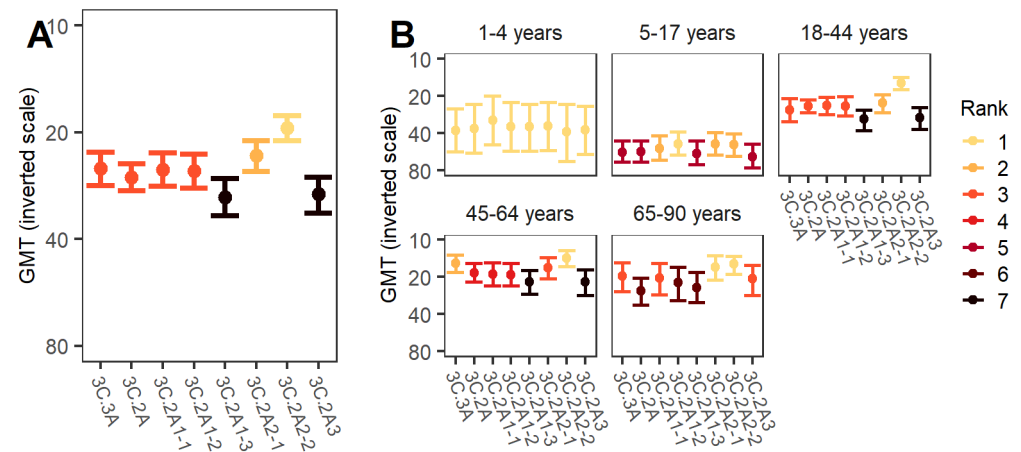
Fig S5. The GMT for each HA reference strain. Since lower GMT corresponds to higher susceptibility, we use an inverse scale to indicate the relative susceptibility. GMTs are shown for the whole population (A) and by age group (B). The bars indicate 95% CIs obtained from bootstrapping. A lower rank indicates significantly higher implied susceptibility: the strain with lowest GMT has rank 1, and strains are tied in rank if their GMTs do not differ significantly.
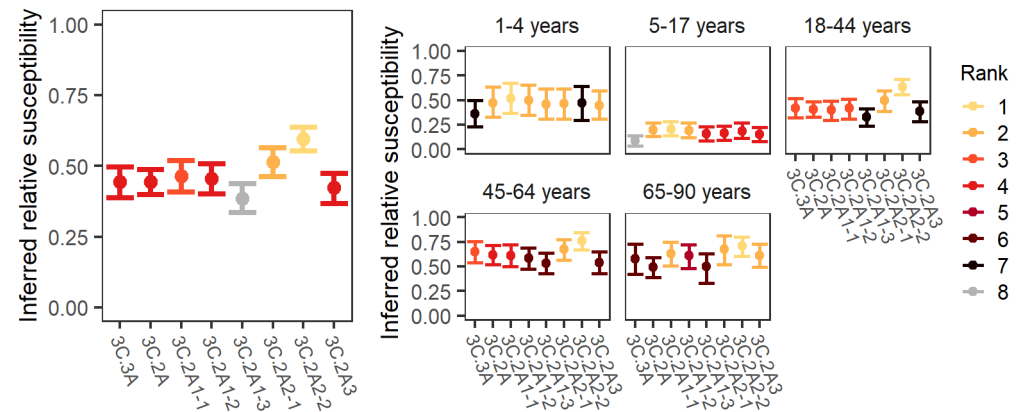

Fig S6. Inferred relative susceptibility to each reference strain using a 1:20 HA titer threshold. Inferred relative susceptibility and the susceptibility rank of each reference strain for the whole population (left) and by age group (right). The bars indicate 95% CIs obtained from bootstrapping. A lower rank indicates significantly higher susceptibility: the strain to which susceptibiity is highest has rank 1, and strains are tied in rank if their relative susceptibilities do not differ significantly.
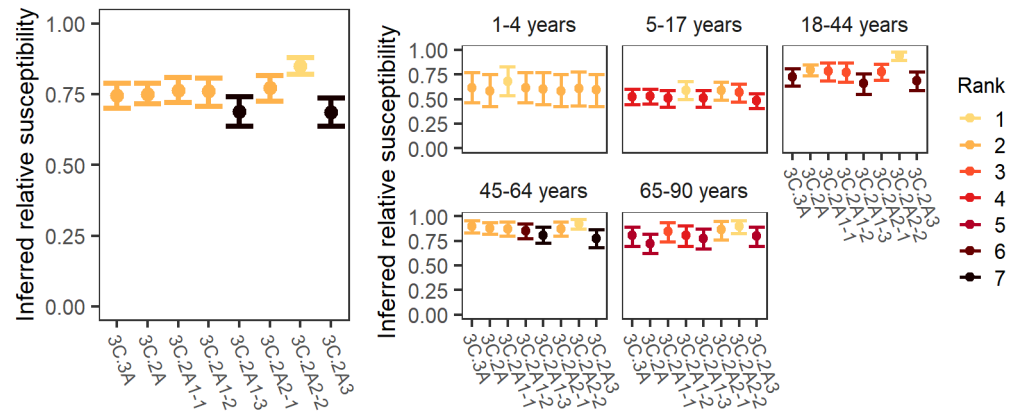
Fig S7. Inferred relative susceptibility to each reference strain using a 1:80 HA titer threshold. Inferred relative susceptibility and the susceptibility rank of each reference strain for the whole population (left) and by age group (right). The bars indicate 95% CIs obtained from bootstrapping. A lower rank indicates significantly higher susceptibility: the strain to which susceptibiity is highest has rank 1, and strains are tied in rank if their relative susceptibilities do not differ significantly.
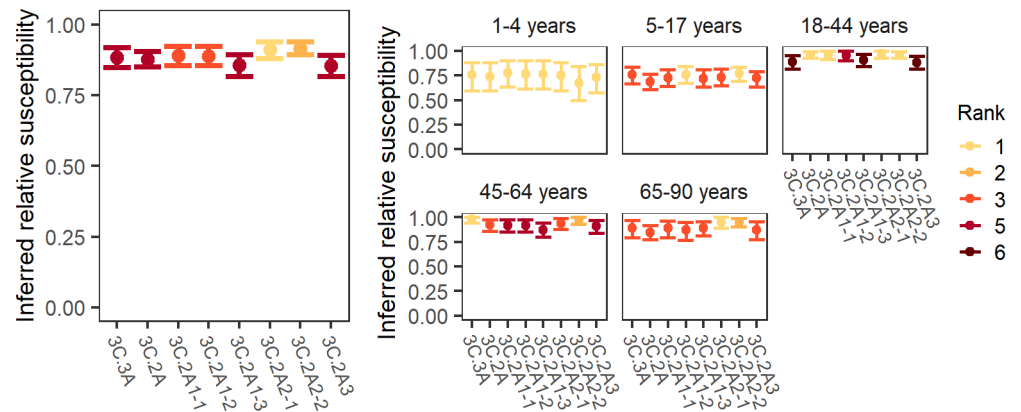

Fig S8. Inferred relative susceptibility to each reference strain using a 1:160 HA titer threshold. Inferred relative susceptibility and the susceptibility rank of each reference strain for the whole population (left) and by age group (right). The bars indicate 95% CIs obtained from bootstrapping. A lower rank indicates significantly higher susceptibility: the strain to which susceptibiity is highest has rank 1, and strains are tied in rank if their relative susceptibilities do not differ significantly.
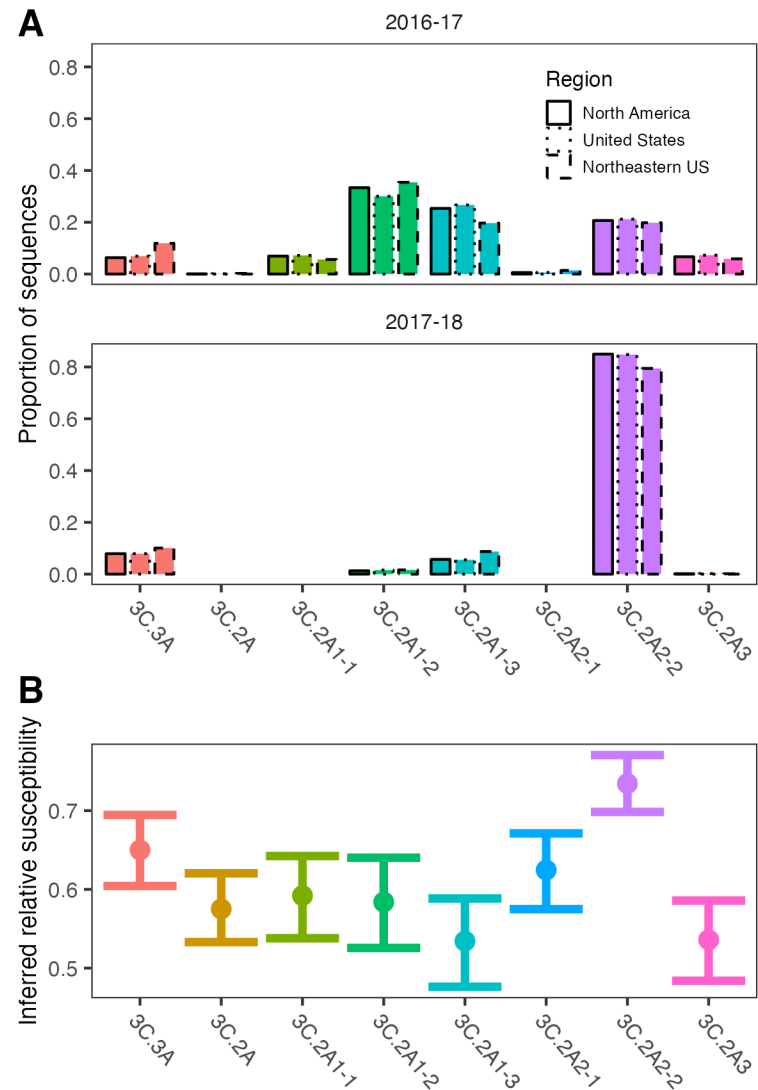
Fig S9. Comparison of H3 proportions by clade (reference strain) and inferred relative susceptibilities. A. Proportion of H3 sequences assigned to each test virus were calculated using GISAID sequences from North America, US, and the Northeastern US during the 2016-17 and 2017-18 season. B. Inferred relative susceptibilities to test viruses assuming a 1:40 HA titer threshold for protection.
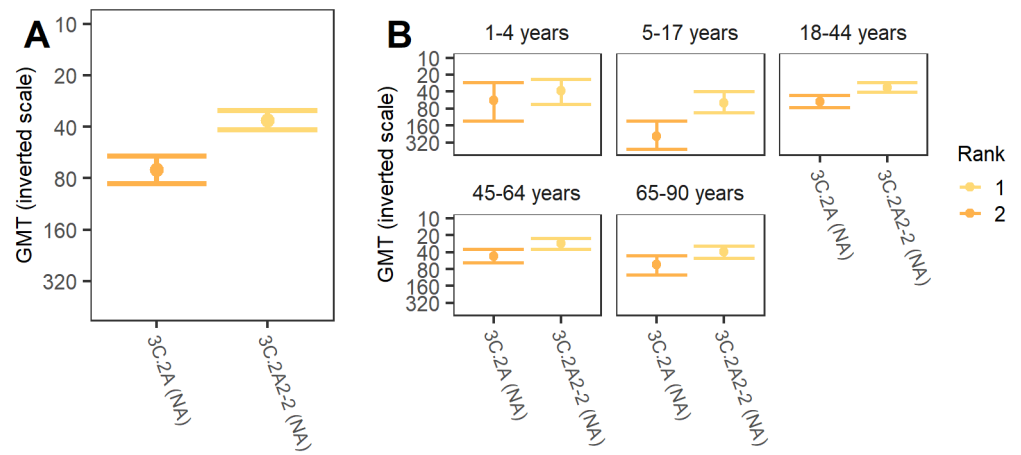
Fig S10. The GMT for each NA reference strain. Since lower GMT corresponds to higher susceptibility, we use an inverse scale to indicate the relative susceptibility. GMTs are shown for the whole population (A) and by age group (B). The bars indicate 95% CIs obtained from bootstrapping. A lower rank indicates significantly higher implied susceptibility: the strain with lower GMT has rank 1.
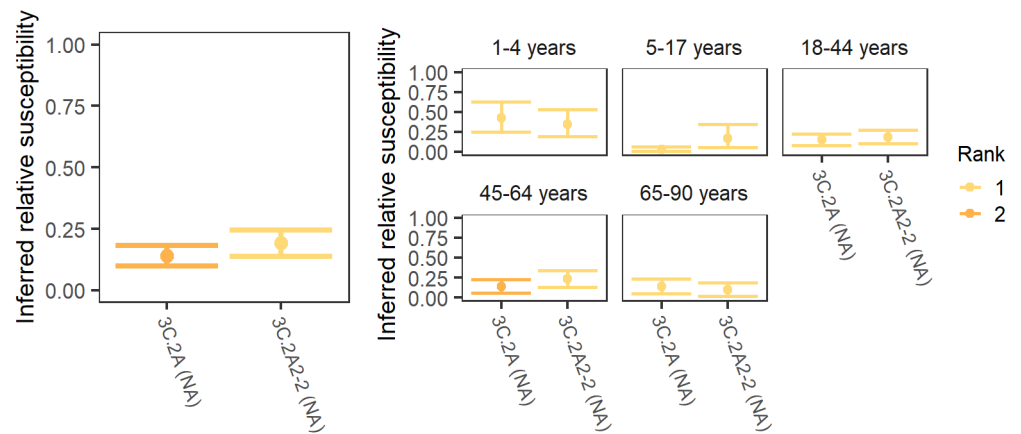

Fig S11. Inferred relative susceptibility to each NA reference strain using a 1:20 threshold. Inferred relative susceptibility and the susceptibility rank of each reference strain for the whole population (left) and by age group (right). The bars indicate 95% CIs obtained from bootstrapping. A lower rank indicates significantly higher susceptibility: the strain to which susceptibiity is highest has rank 1, and strains are tied in rank if their relative susceptibilities do not differ significantly.
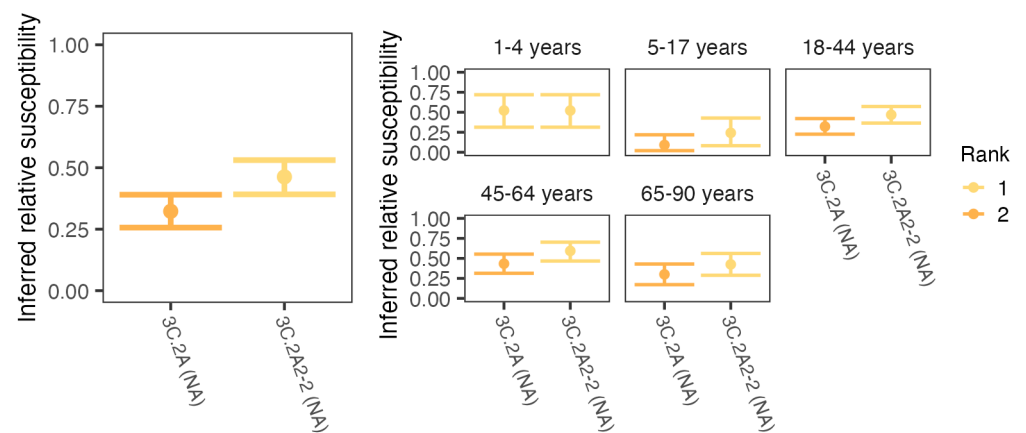
**Fig S12. The inferred relative susceptibility to each reference strain using a
1:40 NA titer threshold.** Inferred relative susceptibility and the susceptibility rank
of each reference strain for the whole population (left) and by age group (right). The
bars indicate 95% CIs obtained from bootstrapping. A lower rank indicates significantly
higher susceptibility: the strain to which susceptibiity is highest has rank 1, and strains
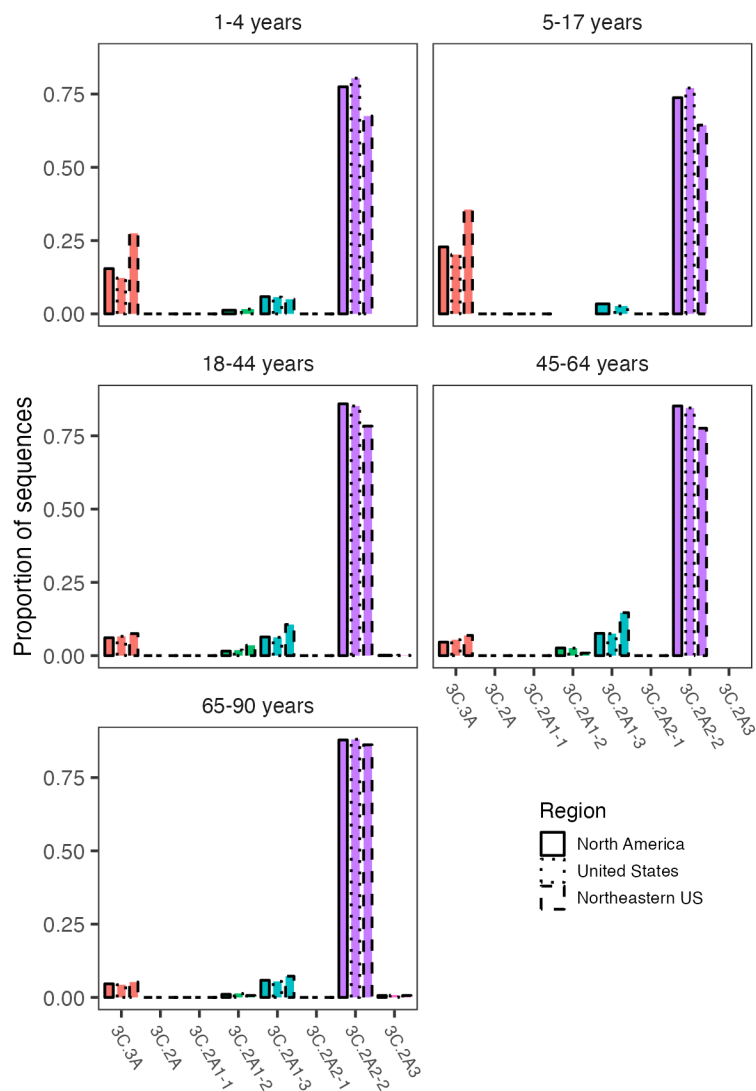are tied in rank if their relative susceptibilities do not differ significantly.

Fig S13. Proportions of H3 sequences in the 2017-18 season assigned to each reference virus by age group. Proportions were calculated using GISAID sequences collected in North America, United States, and the northeastern United States, respectively.
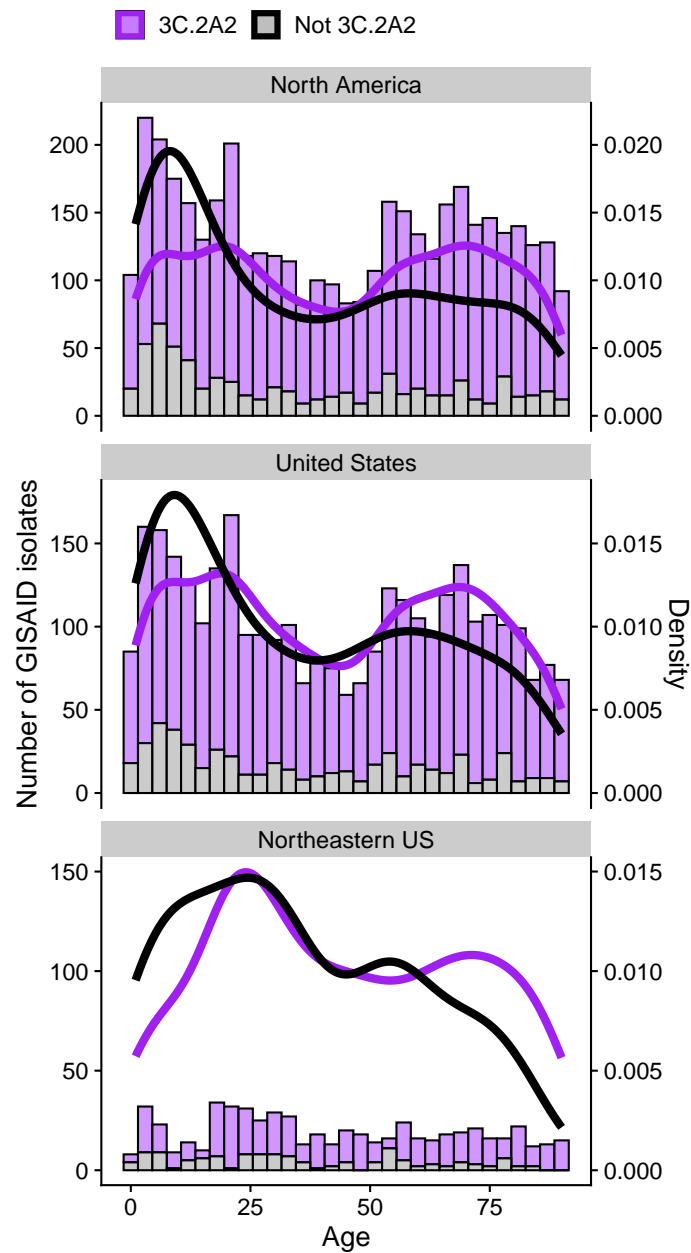
Fig S14. Host age distribution of H3N2 isolates sampled during the 2017/18 season, shown at different geographical resolutions. We obtained isolate data from GISAID. Viruses from clade 3C.2A2 are shown in purple, and viruses from all other clades combined are shown in gray.
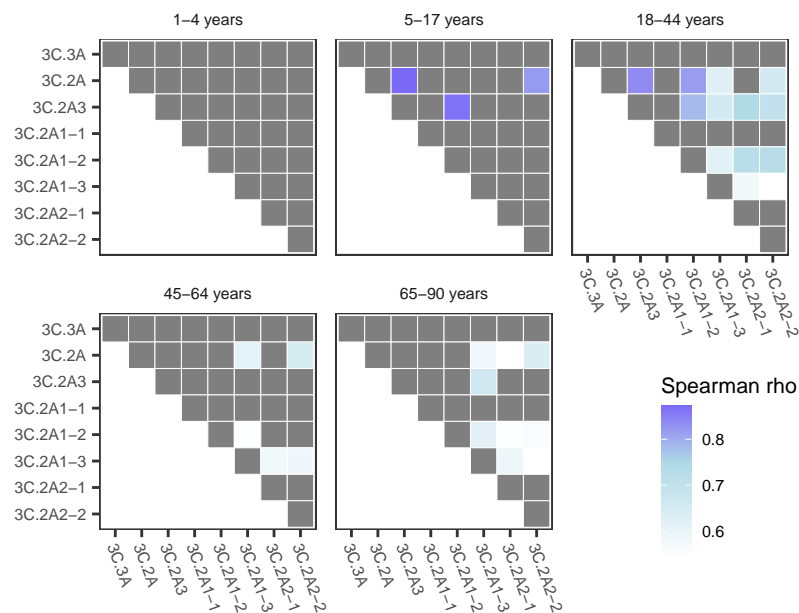
Fig S15. Compared to the youngest age group, older children and adults have significantly more weakly correlated titers to different strains. For each pair of viruses, we calculated the correlation in HA titers within each age group, averaging across 1000 random imputations of continuous titers. For each pair of strains, we used bootstrapping to test if the correlation for that pair in each age group was significantly weaker than in 1-4 year-olds. The cells are colored blue if the correlation is significantly weaker. Individuals with all undetectable titers were removed from these analyses.
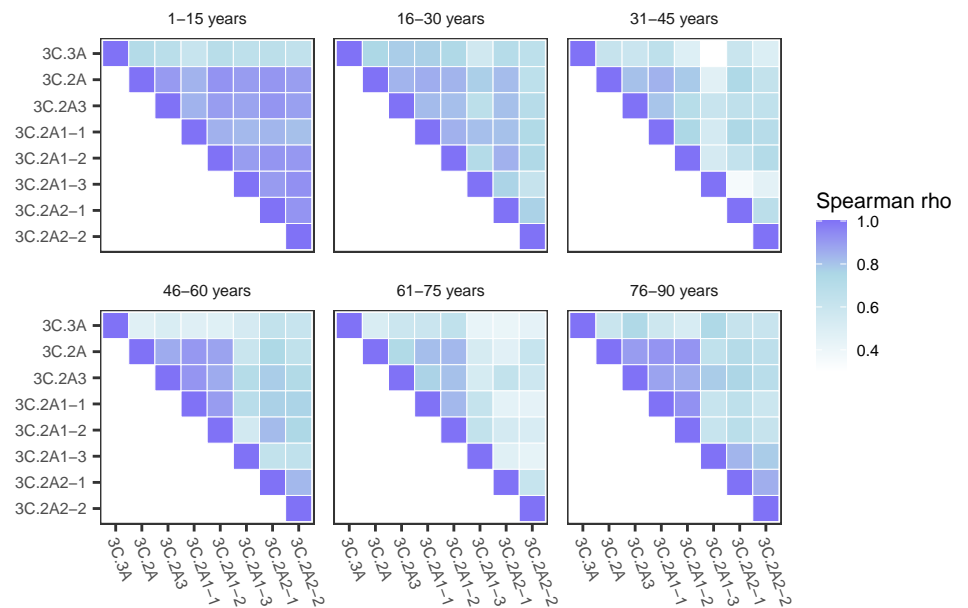
Fig S16. Weak correlations in adults' HA titers between viral strains persist when age groups cover the same number of years. For these analyses, we randomly imputed continuous titer values between consecutive dilutions (e.g., a titer of 160 was replaced by a continuous value between 160 and 320 drawn with uniform probability). For each pair of viruses and each age group, we report the average Spearman correlation coefficient across 1000 replicate imputations. We removed individuals with all undetectable titers from this analysis.
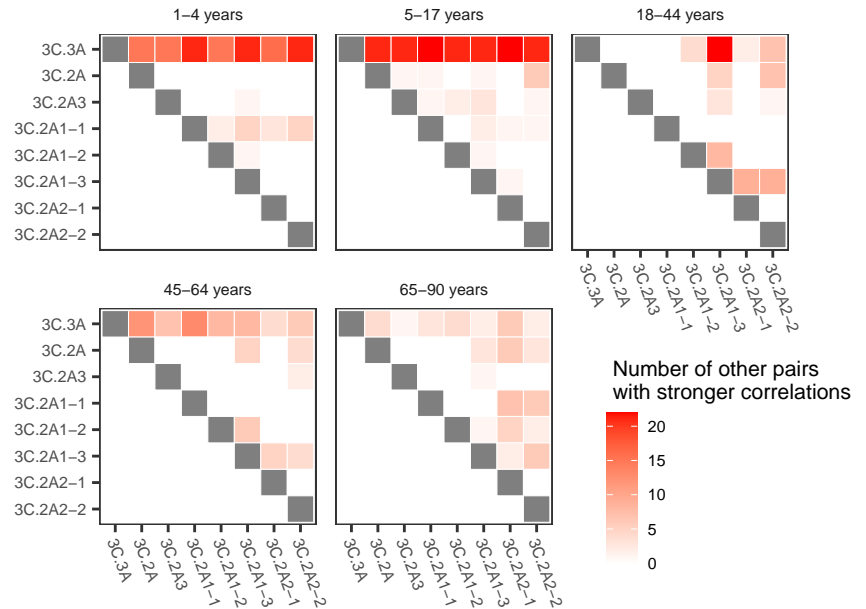
Fig S17. Titers to the 3C.3A virus had the weakest correlation with titers to other viruses. For each pair of viruses, we computed the correlation in HA titers in each age group, averaging across 1000 random imputations of continuous titer values. Within each age group, we used bootstrapping to compare the correlations across different pairs of strains. For each pair of strains, we counted how many other pairs of strains had significantly stronger correlations in the same age group. Strain pairs with weaker correlation than most other pairs appear in dark red. Individuals with all undetectable titers were removed from these analyses. Gray cells indicate the diagonal, where tests were not performed because the correlation is always 1